

## Ultraviolet anti-Stokes photoluminescence in $\text{In}_x\text{Ga}_{1-x}\text{N}/\text{GaN}$ quantum-well structures

Akihiro Satake and Yasuaki Masumoto

*Institute of Physics, University of Tsukuba, Tsukuba, Ibaraki 305-8571, Japan*

Takao Miyajima, Tsunenori Asatsuma, and Tomonori Hino

*Sony Corporation Research Center, Yokohama, Kanagawa 240-0036, Japan*

(Received 30 December 1999)

Ultraviolet anti-Stokes photoluminescence (PL) is observed in  $\text{In}_x\text{Ga}_{1-x}\text{N}/\text{GaN}$  multiple quantum wells. The observed anti-Stokes PL exhibits a quadratic dependence on the excitation energy density. Anti-Stokes PL excitation spectrum is proportional to the optical absorption spectrum of the  $\text{In}_x\text{Ga}_{1-x}\text{N}$  quantum wells. Time-resolved PL measurement shows that a decay of the anti-Stokes PL is slower than that of the GaN PL under the excitation above the band gap of the GaN barrier, and it is half the time constant of the  $\text{In}_x\text{Ga}_{1-x}\text{N}$  PL decay. A two-step two-photon absorption process is directly observed by means of two-color pump-and-probe experiment. It is considered that the anti-Stokes PL is caused by a two-step two-photon absorption process involving a localized state in the  $\text{In}_x\text{Ga}_{1-x}\text{N}$  quantum wells as the intermediate state, and that the second absorption step is provided by photon recycling of the  $\text{In}_x\text{Ga}_{1-x}\text{N}$  PL.

Anti-Stokes photoluminescence (PL) or up-converted PL is a phenomenon in which the photon energy of PL is higher than the excitation photon energy. Generally, the energy up-conversion in bulk semiconductors is achieved by a momentum converting Auger process,<sup>1-3</sup> thermal population of phonon modes observed as anti-Stokes Raman lines,<sup>4,5</sup> or nonlinear mechanisms such as second-harmonic generation, optical parametric oscillation, and two-photon absorption (TPA) processes.<sup>6-8</sup> The TPA processes are classified into a coherent TPA, where the intermediate states are virtual states, and a two-step TPA, where the intermediate states are real states.

Recently, efficient anti-Stokes PL has been observed in heterostructures and quantum wells (QW's) of semiconductors.<sup>9-16</sup> It has been proposed that the carrier excitation mechanisms in anti-Stokes PL are cold Auger process for  $\text{InP}/\text{Al}_x\text{In}_{1-x}\text{As}$  type-II heterojunctions,<sup>9</sup> two-step TPA for  $\text{CdTe}/\text{Cd}_x\text{Mn}_{1-x}\text{Te}$  QW's,<sup>10</sup> and cold Auger process and/or two-step TPA for  $\text{GaAs}/(\text{Al},\text{Ga})\text{InP}_2$  heterostructures.<sup>11-16</sup> In these cases, the samples consist of stacked narrow-gap and wide-gap semiconductors. It has been argued that anti-Stokes PL is caused by a radiative recombination in the wide-gap material, into which carriers are excited from the narrow-gap material. Hellmann *et al.* have proposed that the anti-Stokes PL in the  $\text{CdTe}/\text{Cd}_x\text{Mn}_{1-x}\text{Te}$  QW's is due to the two-step TPA process involving localized or impurity bound exciton state as the intermediate state. The photons for the second absorption step can be provided by the photon recycling of the exciton recombination in the QW's.<sup>10</sup> Driessen *et al.* have proposed that the anti-Stokes PL in  $\text{GaAs}/\text{GaInP}_2$  QW's is due to the cold Auger process via interface states.<sup>11</sup>

In this paper, we report on the observation of ultraviolet anti-Stokes PL in  $\text{In}_x\text{Ga}_{1-x}\text{N}/\text{GaN}$  multiple quantum wells (MQW's). This anti-Stokes PL has the highest photon energy (3.49 eV) in semiconductors to our knowledge. The anti-Stokes PL exhibits a superlinear dependence on the excitation energy density. We demonstrate that the anti-Stokes PL

is due to the two-step TPA process by means of a time-resolved PL measurement and a two-color pump-and-probe experiment.

The sample was Si-doped  $\text{In}_x\text{Ga}_{1-x}\text{N}/\text{GaN}$  MQW's grown on a (0001)-orientated sapphire substrate by a metal-organic chemical vapor deposition. The  $\text{In}_x\text{Ga}_{1-x}\text{N}/\text{GaN}$  MQW's consisted of three periods of a 3.5-nm-thick  $\text{In}_x\text{Ga}_{1-x}\text{N}$  quantum well separated by a 7-nm-thick GaN barrier. The indium concentration of the well was 6.2–7.4% estimated by the x-ray diffraction measurement. The sample consisted of a GaN buffer layer, an undoped GaN layer 1.2  $\mu\text{m}$  thick, a Si-doped GaN 0.8  $\mu\text{m}$  thick, Si-doped  $\text{In}_x\text{Ga}_{1-x}\text{N}/\text{GaN}$  MQW's and a Si-doped GaN layer 100 nm thick. The doping density was about  $2 \times 10^{19} \text{ cm}^{-3}$ . The sample was directly immersed in liquid nitrogen at 77 K.

For optical experiments, the excitation laser source was a mode-locked Ti:sapphire laser (82 MHz, 2 ps) or an optical parametric amplification (OPA) with a Ti:sapphire regenerative amplifier (200 kHz, 300 fs). The excitation for the anti-Stokes PL measurements was performed by a frequency-doubled Ti:sapphire laser output. Under the excitation above the band gap of the GaN barrier, a frequency-doubled OPA output was used. Time-resolved PL profiles were measured by using a synchroscan streak camera connected to a 25-cm subtractive dispersion double monochromator. The time resolution was about 30 ps. A two-color pump-and-probe experiment was performed in the transmission geometry. A part of Ti:sapphire laser pulses were used as the probe beam and the frequency-doubled Ti:sapphire laser pulses were used as the pump beam. The amplitude modulation of the pump beam and probe beam at each frequency (1.5 MHz or 200 Hz) was made by an acousto-optical modulator and a mechanical chopper, respectively. A double lock-in detection of the signal allowed us to reduce noise from the scattered light and to achieve highly sensitive detection of nonlinear transmission. The time dependence of the pump-and-probe signal was measured by scanning the optical delay line.

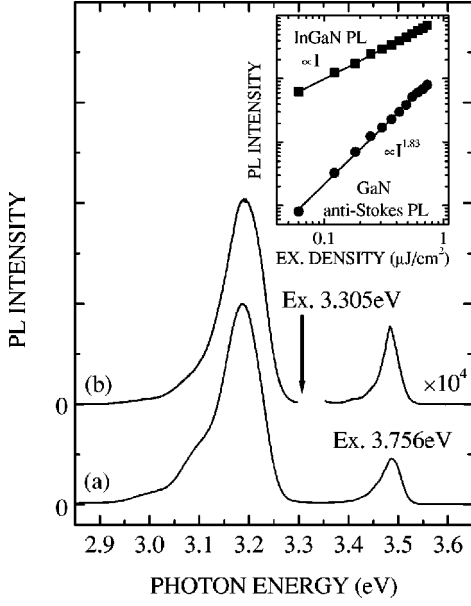


FIG. 1. PL spectra of the  $\text{In}_x\text{Ga}_{1-x}\text{N}/\text{GaN}$  MQW's excited above (a) and below (b) the band gap of the GaN barrier, respectively. The inset shows the excitation energy density dependencies of the  $\text{In}_x\text{Ga}_{1-x}\text{N}$  PL (squares) and GaN anti-Stokes PL intensities (circles), respectively. The excitation photon energy is 3.305 eV.

Figure 1 shows the PL spectra of the  $\text{In}_x\text{Ga}_{1-x}\text{N}/\text{GaN}$  MQW's under the excitation above (a) and below (b) the band gap of the GaN barrier. Under the excitation photon energy at 3.756 eV, we can observe two emission bands. The peak at 3.18 eV is due to the radiative recombination in the  $\text{In}_x\text{Ga}_{1-x}\text{N}$  QW's, while the peak at 3.49 eV is due to that in the GaN barrier. It is a typical PL spectrum of  $\text{In}_x\text{Ga}_{1-x}\text{N}/\text{GaN}$  MQW's system. It has been reported that the low-energy PL is attributed to the recombination of excitons localized at certain potential minima in  $\text{In}_x\text{Ga}_{1-x}\text{N}$  layers.<sup>17–20</sup> The PL intensity of the GaN barrier is smaller than that of the  $\text{In}_x\text{Ga}_{1-x}\text{N}$  QW's, indicating efficient carrier transfer from the GaN barrier into the  $\text{In}_x\text{Ga}_{1-x}\text{N}$  QW's. Under the excitation photon energy at 3.305 eV, a similar  $\text{In}_x\text{Ga}_{1-x}\text{N}$  PL spectrum is observed and an anti-Stokes PL spectrum of the GaN barrier can be observed even under the excitation below the band gap of the GaN barrier. The excitation energy density dependencies of the anti-Stokes PL and the  $\text{In}_x\text{Ga}_{1-x}\text{N}$  PL are shown in the inset of Fig. 1. The anti-Stokes PL exhibits a superlinear dependence ( $\propto I_{ex}^{1.83}$ ) on the excitation density, while the  $\text{In}_x\text{Ga}_{1-x}\text{N}$  PL exhibits linear dependence.

The dependencies of the anti-Stokes PL and  $\text{In}_x\text{Ga}_{1-x}\text{N}$  PL intensities on the excitation photon energy, i.e., the PL excitation (PLE) spectra detected at the anti-Stokes GaN PL band (3.49 eV) and the  $\text{In}_x\text{Ga}_{1-x}\text{N}$  PL band (3.10 eV), are shown in Fig. 2. Because the  $\text{In}_x\text{Ga}_{1-x}\text{N}$  PLE spectrum is almost proportional to the joint density of states in the direct transition type semiconductors and the  $\text{In}_x\text{Ga}_{1-x}\text{N}$  absorption is broadened by  $\sigma = 35$  meV due to the formation of the tail states,<sup>20</sup> the  $\text{In}_x\text{Ga}_{1-x}\text{N}$  PLE spectrum is fitted by the error function

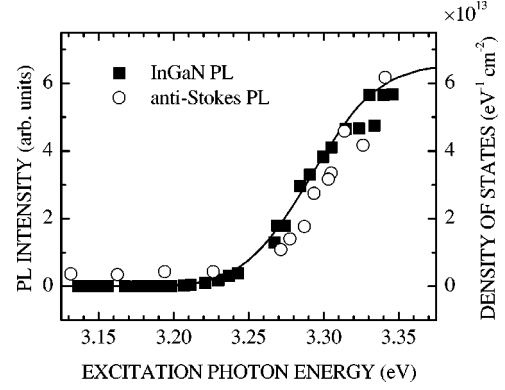


FIG. 2. Excitation photon energy dependencies of the  $\text{In}_x\text{Ga}_{1-x}\text{N}$  PL (closed squares) and GaN anti-Stokes PL intensities (open circles), respectively. The excitation energy density is fixed at  $0.488 \mu\text{J}/\text{cm}^2$ . A solid line is a fitting by Eq. (1) in the text.

$$D(E) = \frac{1}{\sqrt{2\pi\sigma}} \frac{m_r}{\pi\hbar^2} \int_{-\infty}^{\infty} \exp\left(-\frac{(E-t)^2}{2\sigma^2}\right) \Theta(t-E_0) dt$$

$$= \frac{1}{\sqrt{2\pi\sigma}} \frac{m_r}{\pi\hbar^2} \int_{-\infty}^E \exp\left(-\frac{(t-E_0)^2}{2\sigma^2}\right) dt. \quad (1)$$

Here,  $m_r$  is a reduced mass of the electron-hole pair and  $m_r/\pi\hbar^2\Theta(t-E_0)$  is a step function, indicating two-dimensional joint density of states in the  $\text{In}_x\text{Ga}_{1-x}\text{N}/\text{GaN}$  MQW's. The fitted energy of  $E_0 = 3.294$  eV is almost consistent with the calculated value of the lowest quantized energy transition in the  $\text{In}_x\text{Ga}_{1-x}\text{N}/\text{GaN}$  MQW's on the finite potential well model. The intensity of anti-Stokes PL excited above 3.27 eV increases drastically with the increase of the excitation photon energy like that of the  $\text{In}_x\text{Ga}_{1-x}\text{N}$  PL. This result shows that the anti-Stokes PL is excited through the real states in the  $\text{In}_x\text{Ga}_{1-x}\text{N}$  QW's. On the other hand, under the excitation below 3.23 eV, the anti-Stokes PL can be observed although the  $\text{In}_x\text{Ga}_{1-x}\text{N}$  PL becomes weak. The anti-Stokes PL excited at 3.23 eV also exhibits a quadratic dependence on the excitation energy density. It seems that the coherent TPA process or the process related to deeper states such as deep acceptor states causes the anti-Stokes PL excited below 3.23 eV.

Considering a quadratic dependence on the excitation energy density and the participation of the real states of the  $\text{In}_x\text{Ga}_{1-x}\text{N}$  QW's, we presume a main mechanism of the anti-Stokes PL to be the two-step TPA process via the localized states in the  $\text{In}_x\text{Ga}_{1-x}\text{N}$  QW's. We explain the process producing anti-Stokes PL as follows. After the initial excitation process, the electron-hole pairs are generated in the  $\text{In}_x\text{Ga}_{1-x}\text{N}$  QW's. They lose their energy quickly, electrons or holes are captured at certain potential minima, and localized excitons are formed, as schematically shown on the left side of Fig. 3. Since the localized states have a very limited spatial extension, the wave function of the localized exciton has contributions from all  $k$  states in the Brillouin zone. Therefore, high-energetic electron-hole pairs can be directly created by second photon absorption without phonon participation, as shown on the right side of Fig. 3. After the second

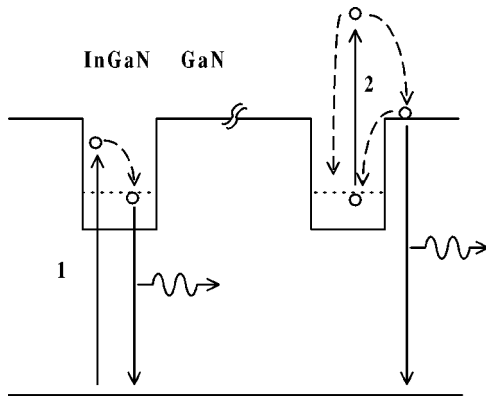


FIG. 3. Schematic illustration of a two-step TPA process for anti-Stokes PL.

excitation process, the electron-hole pairs with the energy higher than the band gap of the GaN barrier relax into the GaN barrier states or are localized again in the  $\text{In}_x\text{Ga}_{1-x}\text{N}$  QW's, and then the electron-hole pairs recombine radiatively like the excitation above the band gap of the GaN barrier. This radiative recombination in the GaN barrier gives rise to the observed anti-Stokes PL.

Time-resolved PL measurement provides us with the carrier dynamics of the  $\text{In}_x\text{Ga}_{1-x}\text{N}/\text{GaN}$  MQW's and shows that the second absorption step is mainly induced by photon recycling, i.e., the photons stem from radiative recombination in the  $\text{In}_x\text{Ga}_{1-x}\text{N}$  QW's. Figures 4(a) and 4(b) show the PL decay profiles under the excitation above and below the band gap of the GaN barrier. Solid lines show the fittings of single or double exponential functions convoluted by the excitation laser profile. The decay profiles of the  $\text{In}_x\text{Ga}_{1-x}\text{N}$  PL (squares) are detected at 3.18 eV, while the decay profiles of the GaN PL (circles) are detected at 3.49 eV. Under the excitation at 3.756 eV, the GaN PL shows a single exponential decay with a decay time constant of 72.1 ps. Then, the

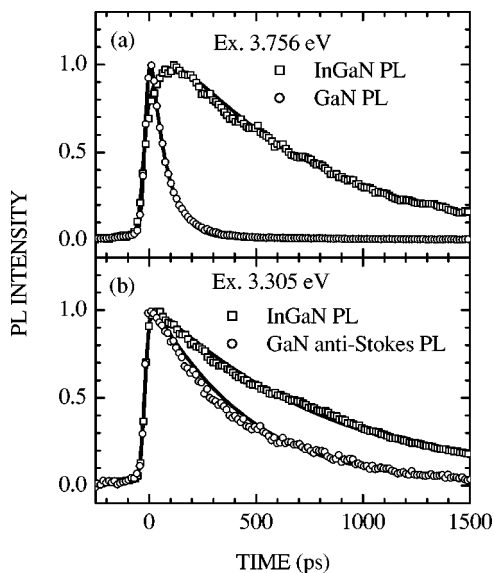


FIG. 4. Temporal changes of the  $\text{In}_x\text{Ga}_{1-x}\text{N}$  PL and the GaN PL excited above (a) and below (b) the band gap of the GaN barrier. These decay profiles are fitted by single or double exponential functions convoluted by the excitation laser profile.

$\text{In}_x\text{Ga}_{1-x}\text{N}$  PL shows 72.1-ps rise and 693-ps decay. The  $\text{In}_x\text{Ga}_{1-x}\text{N}$  PL excited at 3.305 eV shows a single exponential decay with a decay time constant of 800 ps. The decay time of the  $\text{In}_x\text{Ga}_{1-x}\text{N}$  PL increases with the decrease of the detected photon energy (0.4 ns at 3.3 eV, 0.9 ns at 3.1 eV) indicating a typical dynamical feature of the exciton localization in  $\text{In}_x\text{Ga}_{1-x}\text{N}$  ternary alloy system.<sup>19,20</sup> The rise cannot be observed under the excitation below the band gap of the GaN barrier, while the rise is clearly observed under the excitation above the band gap of the GaN barrier. This result indicates that the photogenerated electron-hole pairs transfer from the GaN barrier into the  $\text{In}_x\text{Ga}_{1-x}\text{N}$  QW's.

The anti-Stokes PL excited at 3.305 eV shows a single exponential decay. Its time constant is 425 ps, which is longer than that of GaN PL decay. This indicates that the carrier generation process is slower than the relaxation process in the GaN barrier—if the carrier generation is fast, such as the coherent TPA process or the two-step TPA process where the second absorption step is caused by laser photons, the anti-Stokes PL should be completed within 72 ps. The notable point is that the decay time of the anti-Stokes PL is almost half the time constant of the  $\text{In}_x\text{Ga}_{1-x}\text{N}$  PL decay. In the two-step TPA process on our model, the intensity of the anti-Stokes PL is proportional to the population of the localized states in the  $\text{In}_x\text{Ga}_{1-x}\text{N}$  QW's,  $N_1(t)$ , and to the number of photons responsible for the second absorption step. If the second absorption step is caused by the photons of the  $\text{In}_x\text{Ga}_{1-x}\text{N}$  PL, the number of photons is directly proportional to  $N_1(t)$ : the intensity of the anti-Stokes PL is proportional to  $N_1(t)^2$ . This can explain notable characteristics of the decay time of the anti-Stokes PL.

At this stage, it is difficult to distinguish between two-step TPA processes provided by photon recycling and Auger pro-

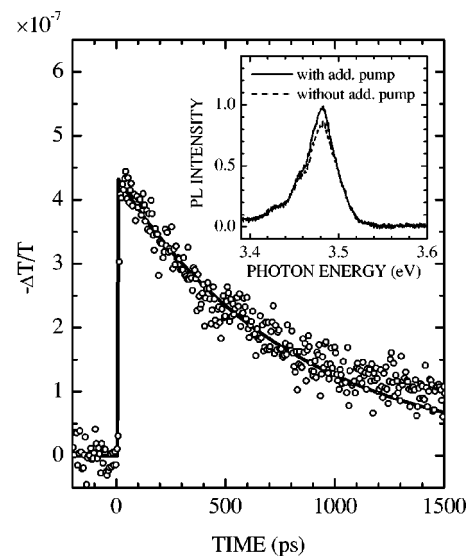


FIG. 5. Temporal change of the differential transmission by means of a two-color pump-and-probe experiment. The photon energy and the excitation energy density of the pump beam are 3.311 eV and  $0.244 \mu\text{J}/\text{cm}^2$ , respectively, while those of the probe beam are 1.656 eV and  $0.049 \mu\text{J}/\text{cm}^2$ , respectively. The inset shows anti-Stokes PL spectra excited at 3.311 eV with (solid line) or without (dashed line) an additional pumping at 1.656 eV. The excitation densities are  $0.146 \mu\text{J}/\text{cm}^2$  for the first pumping and  $0.244 \mu\text{J}/\text{cm}^2$  for the additional pumping, respectively.

cess: the energy transfer due to radiative or nonradiative recombination in the  $\text{In}_x\text{Ga}_{1-x}\text{N}$  QW's. We further performed a two-color pump-and-probe experiment to discuss the second absorption process. In this experiment, the localized excitons are generated in the  $\text{In}_x\text{Ga}_{1-x}\text{N}$  QW's by the pump beam (photon energy below the GaN band gap), and the second photons are supplied by the probe beam (photon energy below the  $\text{In}_x\text{Ga}_{1-x}\text{N}$  band gap). Figure 5 shows a temporal change of the differential transmission. The signal indicates an induced absorption and its decay time is 802 ps, which is comparable to that of the  $\text{In}_x\text{Ga}_{1-x}\text{N}$  PL. The signal is proportional to the intensity of the pump beam. This is the direct observation of the two-step TPA process. This decay profile also assures that the intermediate states are the localized states in the  $\text{In}_x\text{Ga}_{1-x}\text{N}$  QW's. The inset of Fig. 5 shows the anti-Stokes PL spectra excited at 3.311 eV with or without an additional pumping at 1.656 eV. It is clearly seen that the anti-Stokes PL intensity increases by the additional pumping, indicating the anti-Stokes PL can be caused by photon absorption.

Finally, we discuss the efficiency of the photon absorption. The dynamics of the anti-Stokes PL process is described by the rate equations

$$\frac{dN_2}{dt} = -\frac{N_2}{\tau_x} - \frac{N_2}{\tau_D} + \frac{\alpha N_1^2}{\tau_1} + \beta N_1 I_{ex}(t), \quad (2)$$

$$\frac{dN_1}{dt} = -\frac{N_1}{\tau_1} + \frac{N_2}{\tau_D} - \frac{\alpha N_1^2}{\tau_1} - \beta N_1 I_{ex}(t), \quad (3)$$

where  $N_2(t)$  is the population in the GaN barrier,  $\tau_{1(2)}$  is the carrier lifetime in the  $\text{In}_x\text{Ga}_{1-x}\text{N}$  (GaN) layer, and  $\tau_D$  is the relaxation time from the GaN barrier to the  $\text{In}_x\text{Ga}_{1-x}\text{N}$

QW's. In each equation, the first term means the main relaxation term including the radiative recombination. The second term means the relaxation from the GaN barrier to the  $\text{In}_x\text{Ga}_{1-x}\text{N}$  QW's. The third and fourth terms mean the photon absorption by the  $\text{In}_x\text{Ga}_{1-x}\text{N}$  PL ( $N_1/\tau_1$ ) and the laser excitation ( $I_{ex}$ ), respectively. These equations can explain our experimental results well. The absorption efficiency by the  $\text{In}_x\text{Ga}_{1-x}\text{N}$  PL photons ( $\alpha N_1$ ) is guessed by the ratio of the time-integrated  $\text{In}_x\text{Ga}_{1-x}\text{N}$  PL to that of anti-Stokes PL. We estimate the coefficient  $\alpha$  to be  $4 \times 10^{-15} \text{ cm}^2$ . The absorption efficiency by the laser photons ( $\beta N_1$ ) is directly measured by the two-color pump-and-probe experiment. We estimate the coefficient  $\beta$  to be  $1.77 \times 10^{-17} \text{ cm}^2$ . The coefficient  $\alpha$  is  $10^2$  times larger than  $\beta$ . The main reason for the discrepancy is ascribed to the different geometric factor. The intermediate states are present in the  $\text{In}_x\text{Ga}_{1-x}\text{N}$  QW's at the spot size of the laser excitation. The PL photons emit in all the directions. If the condition of total reflection is satisfied, the emission goes back and forth in the lateral direction of the sample. The critical angle for the interface with the GaN buffer and the sapphire substrates is about  $41^\circ$ . Considering the width of the sample (a few  $\mu\text{m}$ ) and the spot size (a few hundred  $\mu\text{m}$ ), the difference between  $\alpha$  and  $\beta$  is reasonably understood.

In summary, we presented detailed experimental studies of ultraviolet anti-Stokes PL in  $\text{In}_x\text{Ga}_{1-x}\text{N}/\text{GaN}$  MQW's. We directly observed second step photon absorption for anti-Stokes PL by means of a two-color pump-and-probe experiment. We conclude that this anti-Stokes PL is mainly caused by a two-step TPA process via localized states of the  $\text{In}_x\text{Ga}_{1-x}\text{N}$  QW's and that the second absorption step can be provided by photon recycling of the  $\text{In}_x\text{Ga}_{1-x}\text{N}$  PL.

- 
- <sup>1</sup>R. Conradt and W. Waidelich, Phys. Rev. Lett. **20**, 8 (1968).  
<sup>2</sup>K. Betzler, Solid State Commun. **15**, 1837 (1974).  
<sup>3</sup>G. Benz and R. Conradt, Phys. Rev. B **16**, 843 (1977).  
<sup>4</sup>R. Loudon, Adv. Phys. **13**, 423 (1964).  
<sup>5</sup>M. Cardona, *Light Scattering in Solid*, Topics in Applied Physics Vol. 8 (Springer, Berlin, 1975).  
<sup>6</sup>Y.R. Shen, *The Principles of Nonlinear Optics* (Wiley, New York, 1984).  
<sup>7</sup>R. Cingolani and K. Ploog, Adv. Phys. **40**, 535 (1991).  
<sup>8</sup>L.G. Quagliano and H. Nather, Appl. Phys. Lett. **45**, 555 (1984).  
<sup>9</sup>W. Seidel *et al.*, Phys. Rev. Lett. **73**, 2356 (1994).  
<sup>10</sup>R. Hellmann *et al.*, Phys. Rev. B **51**, 18 053 (1995).  
<sup>11</sup>F.A.J.M. Driessen *et al.*, Appl. Phys. Lett. **67**, 2813 (1995); Phys. Rev. B **54**, R5263 (1996).  
<sup>12</sup>Z.P. Su, K.L. Teo, P.Y. Yu, and K. Uchida, Solid State Commun. **99**, 933 (1996).  
<sup>13</sup>J. Zeman, G. Martinez, P.Y. Yu, and K. Uchida, Phys. Rev. B **55**, R13 428 (1997).  
<sup>14</sup>Y.-H. Cho *et al.*, Phys. Rev. B **56**, R4375 (1997).  
<sup>15</sup>K. Yamashita, T. Kita, and T. Nishino, J. Appl. Phys. **84**, 359 (1998).  
<sup>16</sup>T. Kita *et al.*, Phys. Rev. B **59**, 15 358 (1999).  
<sup>17</sup>M. Smith *et al.*, Appl. Phys. Lett. **69**, 2837 (1996).  
<sup>18</sup>S. Chichibu *et al.*, Appl. Phys. Lett. **69**, 4188 (1996); **70**, 2822 (1997).  
<sup>19</sup>Y. Narukawa *et al.*, Phys. Rev. B **55**, R1938 (1997); Appl. Phys. Lett. **70**, 981 (1997).  
<sup>20</sup>A. Satake *et al.*, Phys. Rev. B **57**, R2041 (1998); **60**, 16 660 (1999).